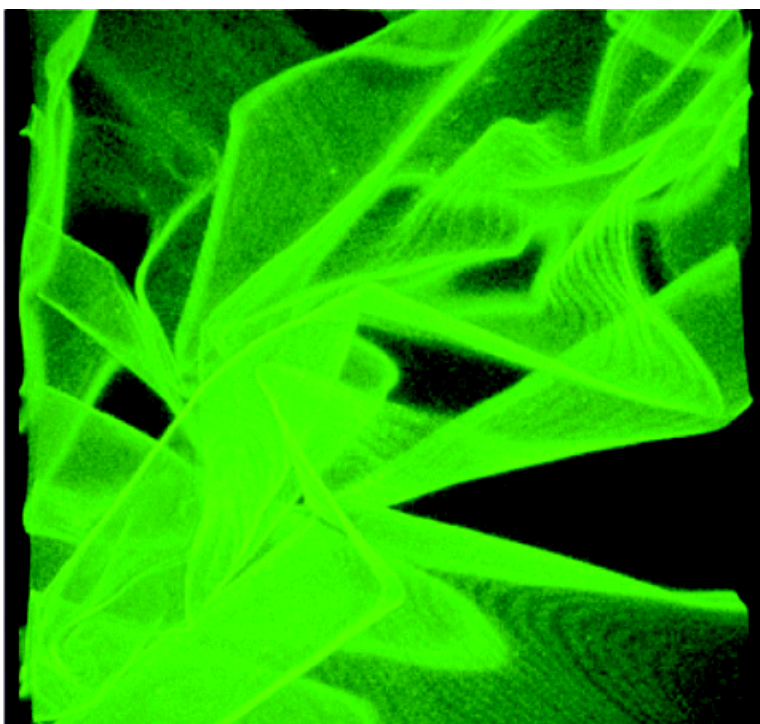


## Ultrathin Cross-Linked Nanoparticle Membranes

Yao Lin, Habib Skaff, Alexander Bker, A. D. Dinsmore, Todd Emrick, and Thomas P. Russell

*J. Am. Chem. Soc.*, **2003**, 125 (42), 12690-12691 • DOI: 10.1021/ja036919a • Publication Date (Web): 27 September 2003

Downloaded from <http://pubs.acs.org> on March 30, 2009



### More About This Article

Additional resources and features associated with this article are available within the HTML version:

- Supporting Information
- Links to the 18 articles that cite this article, as of the time of this article download
- Access to high resolution figures
- Links to articles and content related to this article
- Copyright permission to reproduce figures and/or text from this article

[View the Full Text HTML](#)



**ACS Publications**  
High quality. High impact.

## Ultrathin Cross-Linked Nanoparticle Membranes

Yao Lin,<sup>†</sup> Habib Skaff,<sup>†</sup> Alexander Böker,<sup>†</sup> A. D. Dinsmore,<sup>\*,‡</sup> Todd Emrick,<sup>\*,†</sup> and Thomas P. Russell<sup>\*,†</sup>

*Polymer Science & Engineering Department, University of Massachusetts Amherst, Amherst, Massachusetts 01003, and Department of Physics, University of Massachusetts Amherst, Amherst, Massachusetts 01003*

Received June 26, 2003; E-mail: dinsmore@physics.umass.edu; tsemrick@mail.pse.umass.edu; russell@mail.pse.umass.edu

Assembly and chemical reactions at interfaces using polymers, surfactants, lipids, and proteins have been well studied.<sup>1–6</sup> However, very few routes independently control mechanical, structural, electronic, and optical properties. Functionalized nanoparticles are ideal for hierarchical self-assembly, as the nanoparticles possess a range of tunable electronic and optical properties,<sup>7–11</sup> while the attached ligands can be tuned to tailor interactions with the surroundings. Fluid/fluid interfaces offer unique platforms for the assembly of colloidal particles.<sup>12–16</sup> Interfaces between immiscible fluids, i.e., on the surface of droplets, have been shown to be ideal for the assembly of elastic, semipermeable capsules composed of micrometer-sized colloidal particles.<sup>15</sup> Recently, we described the self-assembly of ligand-stabilized nanoparticles at fluid/fluid interfaces and phase separation of different sized nanoparticles on the interface.<sup>16</sup> The weak interfacial confinement of nanoparticles relative to micrometer-sized particles led to particle-size-dependent self-assembly and exchange at the fluid/fluid interface.

For optimal utilization of nanoparticles at fluid interfaces, methods are needed to provide robust assemblies so that the interface can be removed after the assembly. Here we describe chemical cross-linking of the ligands attached to the nanoparticles as an effective route to this end. The ability to functionalize the ligands and provide rapid diffusion of reagents to the fluid/fluid interface allows stabilization of the nanoparticle assemblies via cross-linking to give nanoparticles embedded in a network of cross-linked ligands. These composite organic–inorganic, nanometer-thick membranes prevent convection but allow diffusion of small molecules across the interface. Compared with layer-by-layer polyelectrolyte deposition,<sup>17</sup> or charged colloidal particles,<sup>18</sup> assembly at the soft fluid/fluid interface requires fewer steps, affords ultrathin membranes of nanoparticle width, and may reduce structural defects due to the mobility of nanoparticles at the fluid interface.

Figure 1a shows a fluorescence confocal microscope image of the air/toluene and toluene/water interfaces with  $4.6 \pm 0.2$  nm diameter tri-*n*-octylphosphine oxide (TOPO)-stabilized CdSe nanoparticles in toluene. As in previous studies,<sup>16</sup> nanoparticle assembly is observed at the toluene/water interface, while there is no noticeable assembly at the toluene/air interface. The diffuse background arises from the nanoparticles dispersed in the toluene phase. Figure 1b shows a fluorescence image of a water droplet in toluene covered with CdSe nanoparticles, while Figure 1c shows the inverse case. The nanoparticles self-assemble so as to form a separating layer between the water and toluene. Studies of dried droplets with atomic force microscopy, transmission electron microscopy, and in situ studies by small-angle X-ray scattering indicate that the nanoparticles form a nearly close-packed monolayer with liquidlike ordering.

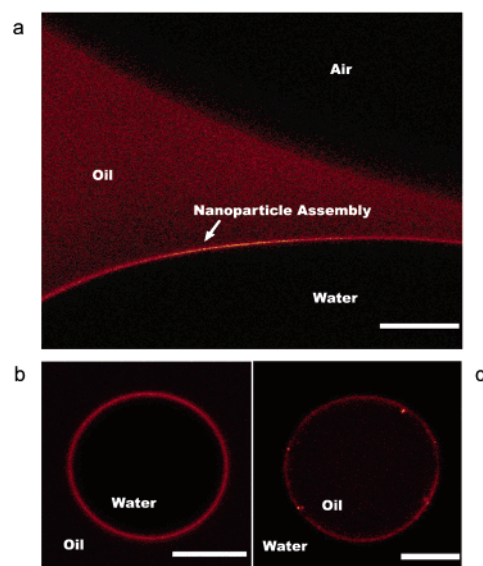


**Figure 1.** Fluorescence confocal microscopy on a nanoparticle assembly where an air bubble was introduced by micropipet, showing (a) preferential segregation of CdSe nanoparticles at the oil/water interface (scale bar 70  $\mu\text{m}$ ) (b) water-in-oil droplets; and (c) oil-in-water droplets (scale bar 20  $\mu\text{m}$ ).

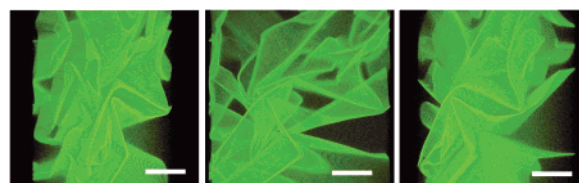


**Figure 2.** Confocal microscope image of a nanoparticle sheet prepared by cross-linking the associated organic ligands. The scale bar is 50  $\mu\text{m}$ .

The dense packing of the ligand-covered nanoparticles at the fluid/fluid interface opens the possibility of stabilizing the assembly by cross-linking the ligands.<sup>19</sup> CdSe nanoparticles with a core diameter of  $2.9 \pm 0.2$  nm and covered with reactive vinylbenzene moieties were prepared as described previously<sup>20</sup> and dispersed in toluene. This solution was introduced to an aqueous solution of 2,2'-azobis(2-(2-imidazolyl)propane) dihydrochloride (Wako VA-044), to give nanoparticle assembly at the planar oil/water interface. The system was sealed under nitrogen and heated to 60  $^{\circ}\text{C}$  for 6 h to afford a membrane of cross-linked nanoparticles at the toluene/water interface. The membrane was removed from the interface by pipet and suspended in toluene.

Figure 2 shows three-dimensional confocal fluorescence microscope images of the resulting sheet suspended in toluene (rotated to view at three different angles). The surface area of the sheet is on the order of 1  $\text{cm}^2$ . The crumpled morphology may result from shear stresses during manipulation with the micropipet. The fluores-

<sup>†</sup> Polymer Science & Engineering Department, University of Massachusetts Amherst.

<sup>‡</sup> Department of Physics, University of Massachusetts Amherst.

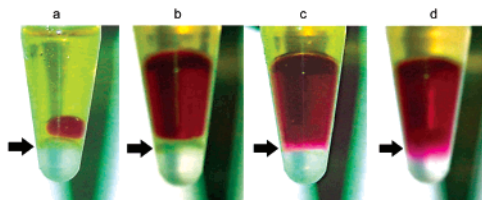


**Figure 3.** Digital photographs of organic dye (red solution) becoming entrapped and then diffusing across a membrane of cross-linked nanoparticles. The bold arrow points to the interface in each tube.

cence emission (excitation: 488 nm, detection: 540 nm) arises from the nanoparticles, unchanged before and after assembly and cross-linking. The observation of a structurally intact membrane floating freely in toluene demonstrates that the ligands attached to the nanoparticles cross-linked into a continuous, elastic membrane. This membrane, while clearly observable by photoluminescence, is invisible in a transmission optical microscope due to its ultrathin nature.

The morphology of the crumpled sheets provides insight into their elastic properties. The pronounced ridges observed in the confocal images are similar to those seen in macroscopic crumpled elastic sheets such as paper or aluminum foil.<sup>21</sup> Elasticity theory characterizes this elastic sheet by an area-expansion modulus  $G$  and a bending modulus  $\kappa$ . If the membrane is composed of an isotropic material, then  $(\kappa/G)^{1/2}$  is approximately equal to the membrane thickness. The ratio of  $\kappa/G$  also determines the morphology of the crumpled sheet<sup>21</sup> and can be measured by comparing the typical curvature,  $C_0$ , and the length,  $L$ , of the ridges as

$$C_0 \approx \left(\frac{1}{L}\right) \left(\frac{L}{(\kappa/G)^{1/2}}\right)^{1/3}$$

From the confocal images, many  $C_0$  and  $L$  pairs were measured to give  $(\kappa/G)^{1/2}$  from 2 to 7 nm, comparable to the membrane thickness ( $\sim 5$  nm). The deformation is consistent with that of a uniform elastic sheet. An upper bound to  $\kappa$  can be obtained by modeling the membrane as a  $\sim 5$ -nm thick layer of polystyrene, which yields  $\kappa \approx 10^5 k_B T$ . While this is an overestimate, it is consistent with the fact that no thermal undulations of the membrane were observed, indicating that  $\kappa$  is at least  $10 k_B T$ .

Permeable and robust sheets of the type shown here have great potential as diffusion barriers. Following sheet formation at the toluene/water interface as described above, a droplet of an aqueous solution of sulforhodamine-B was placed on top of the membrane. Figure 3a shows the membrane's ability to support the droplet. The curvature of the membrane arises from its contact with the side walls of the tube and the energies of the toluene/water, toluene/wall, and water/wall interfaces. Additional dye solution was then added (Figure 3b), and the tube was tapped vigorously to spread the dye across the membrane and to remove toluene trapped between the dye and the membrane. This resulted in a decreased curvature of the membrane (Figure 3c) but no convective transport of the dye across the membrane. After 12 min the dye had diffused across the nanoparticle membrane and into the water phase (Figure 3d).

It should be noted that the diffusion front of the dye in the water is fairly sharp, indicating an absence of convection current in the water phase. In control experiments using non-crosslinked assemblies of CdSe nanoparticles, the dye solution penetrated the nanoparticle assembly by convection, immediately dispersing the sulforhodamine-B in the water at the base of the tube. These results point to the robust barrier properties of the nanoparticle membrane and their ability to prevent convective mixing. They also show that the membrane is permeable, yet may serve to retard or suppress the diffusion of larger molecules across the layer.

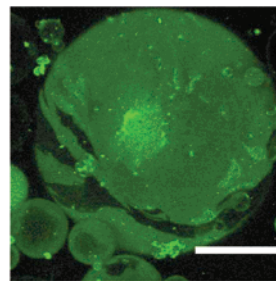


**Figure 4.** Confocal microscope image of a water droplet dispersed in toluene covered by a shell of cross-linked CdSe nanoparticles. The scale bar is 40  $\mu\text{m}$ .

Cross-linking of the ligands can also be used to stabilize the nanoparticle assembly on the interface of droplets. This leads to the encapsulation of the water droplets by a shell of cross-linked nanoparticles. Subsequent centrifugation and washing with pure toluene caused some of the cross-linked shells to crack, as shown in Figure 4. Nevertheless, the integrity of the assembly is maintained, showing the impact of ligand cross-linking in promoting the mechanical and structural stability of the assemblies.

In summary, self-assembly of chemically functionalized nanoparticles at the toluene/water interface, coupled with chemical cross-linking of the attached ligands, provides a simple and flexible route for the fabrication of ultrathin, composite organic-inorganic membranes. Interfacial cross-linking at droplet surfaces enables the encapsulation of water-soluble or oil-soluble materials inside the resulting nanocontainers. By varying the concentration of reactive moieties, it will be possible to control the permeability and strength of these nanostructured membranes.

**Acknowledgment.** This work was supported by the DOE (DE-FG-02-96ER45), the NSF supported MRSEC at UMass Amherst (DMR 9400488), an NSF Career Award (CHE-0239486), the Eastman Kodak Company and the MAX KADE Foundation. We are grateful for stimulating discussions with Profs. A. J. Levine and N. Menon.

## References

- (1) Lasic, D. D. *Liposomes: from Physics to Applications*; Elsevier: Amsterdam, 1993.
- (2) Discher, B. M.; Won, Y. Y.; Ege, D. S.; Lee, J. C. M.; Bates, F. S.; Discher, D. E.; Hammer, D. A. *Science* **1999**, *284*, 1143.
- (3) Koltover, I.; Salditt, T.; Rädler, J. O.; Safinya, C. R. *Science* **1998**, *281*, 78.
- (4) Hackl, W.; Barmann, M.; Sackmann, E. *Phys. Rev. Lett.* **1998**, *80*, 1786.
- (5) Sackmann, E. *Science*, **1996**, *271*, 43.
- (6) Huo, Q.; Margolese, D. I.; Ciesla, U.; Demuth, D. G.; Feng, P. Y.; Gier, T. E.; Sieger, P.; Firouzi, A.; Chmelka, B. F.; Schüth, F.; Stucky, G. D. *Chem. Mater.* **1994**, *6*, 1176.
- (7) Brus, L. *Appl. Phys. A* **1991**, *A53*, 465.
- (8) Alivisatos, A. P. *Science* **1996**, *271*, 933.
- (9) Lenglet, J.; Borudon, A.; Bacri, J. C.; Perzynski, R.; Demouch, G. *Phys. Rev. B* **1996**, *53*, 14941.
- (10) Alivisatos, A. P.; Barbara, P. F.; Castleman, A. W.; Chang, J.; Dixon, D. A.; Klein, M. L.; McLendon, G. L.; Miller, J. S.; Ratner, M. A.; Rossy, P. J.; Stupp, S. I.; Thompson, M. E. *Adv. Mater.* **1998**, *10*, 1297.
- (11) Trindale, T.; O'Brien, P.; Pickett, N. L. *Chem. Mater.* **2001**, *13*, 3843.
- (12) Gaudin, A. M. *Flotation*; McGraw-Hill, Inc.: New York, 1957.
- (13) Pieranski, P. *Phys. Rev. Lett.* **1980**, *45*, 569.
- (14) Velev, O. D.; Furusawa, K.; Nagayama, K. *Langmuir* **1996**, *12*, 2374.
- (15) Dinsmore, A. D.; Hsu, M. F.; Nikolaidis, M. G.; Marquez, M.; Bausch, A. R.; Weitz, D. A. *Science* **2002**, *298*, 1006.
- (16) Lin, Y.; Skaff, H.; Emrick, T.; Dinsmore, A. D.; Russell, T. P. *Science* **2003**, *299*, 226.
- (17) Decher, G. *Science* **1997**, *277*, 1232.
- (18) Caruso, F.; Caruso, R. A.; Möhwald, H. *Science* **1998**, *282*, 1111.
- (19) Ford, J. F.; Vickers, T. J.; Mann, C. K.; Schlenoff, J. B. *Langmuir* **1996**, *12*, 1944.
- (20) Skaff, H.; Ilker, M. F.; Coughlin, E. B.; Emrick, T. *J. Am. Chem. Soc.* **2002**, *124*, 5729.
- (21) Lobkovsky, A.; Gentges, S.; Li, H.; Morse, D.; Witten, T. *Science* **1995**, *270*, 1482.

JA036919A